Oil Shale, 2019, Vol. 36, No. 2S, pp. 128–141
doi: https://doi.org/10.3176/oil.2019.2S.04
ISSN 0208-189X

PHENOLS TO PORES TO ADSORPTION

A POTENTIAL ROUTE TOWARDS NEW METHODS FOR EXTRACTING VALUE FROM SHALE OIL SIDE STREAM

ALLAN NIIDU*

Department of Chemistry and Biotechnoloy, Tallinn University of Technology, Ehitajate tee 5, 19086 Tallinn, Estonia

Abstract. *A side stream of shale oil production contains alkylresorcinols as main constituents, which could prove to be useful intermediates to highly porous and versatile materials – metal-organic frameworks (MOFs). The latter structures have been used as adsorbents for various organic and inorganic compounds, including organic sulfur containing molecules. In the current work, a pathway from phenolic compounds in shale oil toward metal-organic framework linkers was indicated and its utility was proved by using related metal-organic frameworks as effective adsorbents for sulfur from model fuels exemplified in the form of benzothiophene (BT) and isooctane, respectively.*

Keywords: *shale oil, alkylresorcinol, metal-organic framework, adsorption, sulfur.*

1. Introduction

Producing shale oil from Estonian oil shale Kukersite is on many occasions accompanied by the production of phenolic compounds, some of which have been commercialized, like 2-methyl resorcinol (2-MR) and 5-methyl resorcinol (5-MR). These compounds are suitable starting compounds for production of porous materials [1] and could provide an easy access to ligands useful in synthesis of metal-organic frameworks (MOFs) [2]. A possible route from recorcinols to the MOF linkers is depicted in Figure 1. The Kolbe-Schmitt reaction of 5-MR leads to carboxylation of resorcinol [3–5] and subsequent aerobic oxidation to terephthalic acid derivative [6, 7]. Carboxylation could be performed also by biochemical means [8, 9]. 3,5-Dihydroxybenzoic acid has been subjected to the Kolbe-Schmitt reaction to get dihydroxyterephthalic acid directly [10, 11].

* Corresponding author: e-mail: *allan.niidu@taltech.ee*

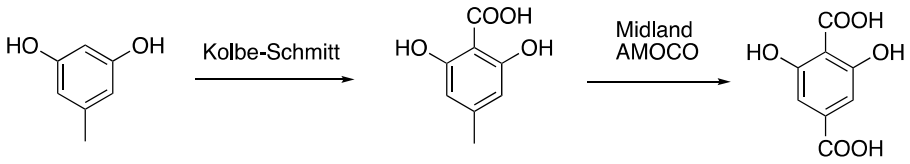

Fig. 1. Pathway from resorcinols to MOF linkers.

These high surface area compounds are extremely versatile materials, being useful as gas separation or storage media, adsorbents to various organic molecules [12], and chemical sensors or catalysts for many chemical processes [13]. Some of said porous materials can be used to remove sulfur containing organic compounds from fuels [14–16]. To model the efficiency of such structures a series of adsorption experiments were conducted demonstrating moderate to excellent capacity in removal of benzothiophene (BT) as a representative organic sulfur compound abundant in shale oils. The Universitetet i Oslo (UIO-66) family MOFs were chosen pertaining to their ease of manufacture [17, 18], excellent thermal [19, 20] and hydrolytic [21] stability [22].

2. Experimental

All chemicals were used as purchased from supplier. The UIO-series MOFs were synthesized according to the known literature procedure by Katz et al. [23] and Rimoldi et al. [24], which leads to 8-connected structures. All synthesized MOF samples were thermally activated under ultra-high vacuum at suitable temperature for at least 12 h on a Micromeritics Smart VacPrep. Nitrogen adsorption and desorption isotherm measurements were performed on a Micromeritics Tristar II at 77K. Powder X-ray diffraction (PXRD) measurements were collected on a STOE STADI MP equipped with a Kα1 radiation source and a 1D strip detector or Rigaku ATXG or Rigaku Smartlab over a range of $2° < 2\theta < 45°$. Scanning electron microscopy (SEM) studies were performed on a Hitachi S4800-II cFEG or SU8030. Gas chromatography (GC) analysis was carried out on an Agilent 7820A fitted with a flame ionization detector (FID) and a DB-5 column.

MOF samples obtained were characterized by nitrogen adsorption isotherms (Fig. 2), Brunauer-Emmet-Teller (BET) surface area and PXRD measurement (Fig. 3), which in all cases were in good agreement with previous results [23, 25]. All produced MOFs except UIO-67 exhibited a broad peak in PXRD spectra in 2θ region from 2° to 5° (Fig. 3), being associated with missing node defects [26, 27].

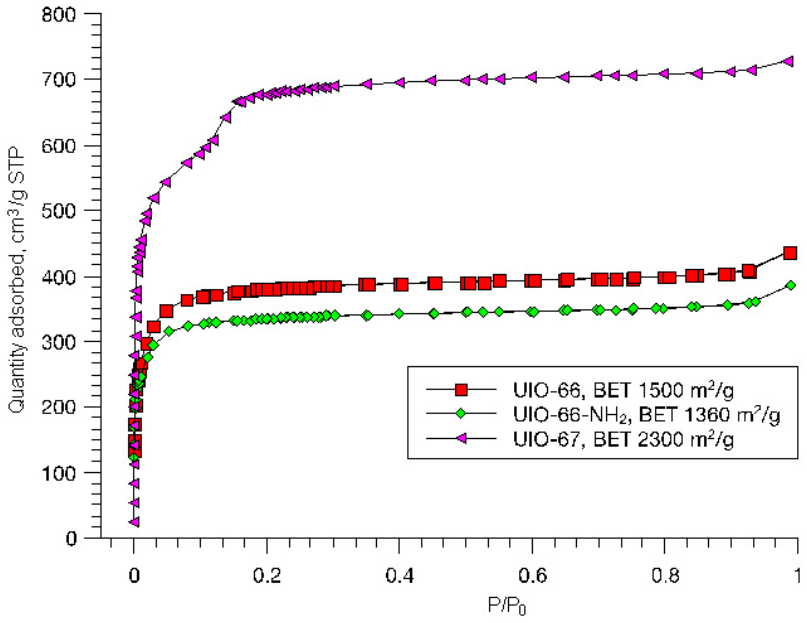

Fig. 2. N_2 adsorption isotherms for UIO-66 series MOFs along with BET surface area values.

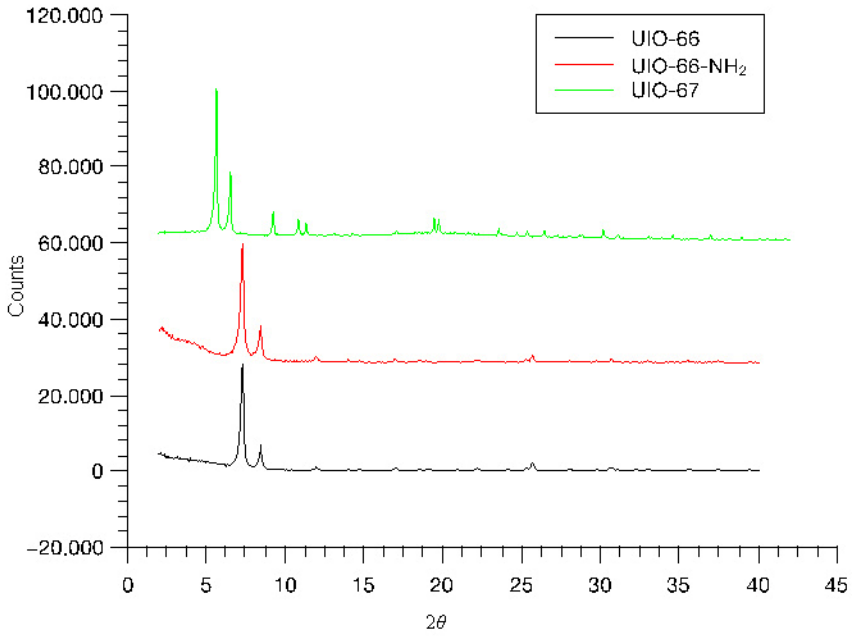

Fig. 3. PXRD of UIO-66 series MOFs.

3. Studies of benzothiophene adsorption on UIO-66 type MOFs

3.1. Kinetics

In a typical experiment 16 to 50 mg of MOF was taken and suspended in a 241 ppmw BT solution in isooctane (5 mL). The mixture was constantly stirred with a magnetic stirrer, only stopped briefly while extracting samples (á 200 μL) at 10, 30, 60 and 120 min, and at 24 h. The samples were centrifuged and analyzed by gas chromatography-flame ionization detector (GC-FID) in isothermal mode.

As can be seen from Figure 4, in all cases the uptake of BT from the isooctane solution was fast and mostly complete after only 10 min of exposure. Kinetic parameters were estimated from linearization of the pseudo second-order kinetic equation (Eq. (1)) (Table 1) [28–30]:

$$\frac{t}{q_t} = \frac{1}{\mathrm{K}_2 q_e^2} + \frac{1}{q_e} t \,, \tag{1}$$

where q_t is the amount adsorbed at time t, $\frac{\mathrm{mg}}{\mathrm{g}}$; t is the time of adsorption, h; q_e is the amount adsorbed at equilibrium, $\frac{\mathrm{mg}}{\mathrm{g}}$; K_2 is the pseudo second-order kinetic constant, $\frac{\mathrm{g}}{\mathrm{mg.h}}$; h is the initial sorption rate, $\frac{\mathrm{mg}}{\mathrm{g.min}}$ and is expressed as follows [28]:

$$h = \mathrm{K}_2 q_e^2. \tag{2}$$

The linear plot and respective fits are represented in Figure 4 and numerical values are presented in Table 2. The highest initial sorption rate was observed for UIO-66-NH_2 and the highest equilibrium uptake at an initial BT concentration of 240 ppmw for UIO-67. R^2 values were high for all the tested MOFs (Table 2).

Table 1. Kinetic parameters obtained from the pseudo second-order kinetic equation

No.	MOF	K_2, g/(mg.min)	h, mg/(g.min)	q_e, mg/g	R^2
1	UIO-66	2.9	1.9	0.8	0.999
2	UIO-66-NH_2	48	654	3.7	1.000
3	UIO-67	0.3	48	13.0	1.000

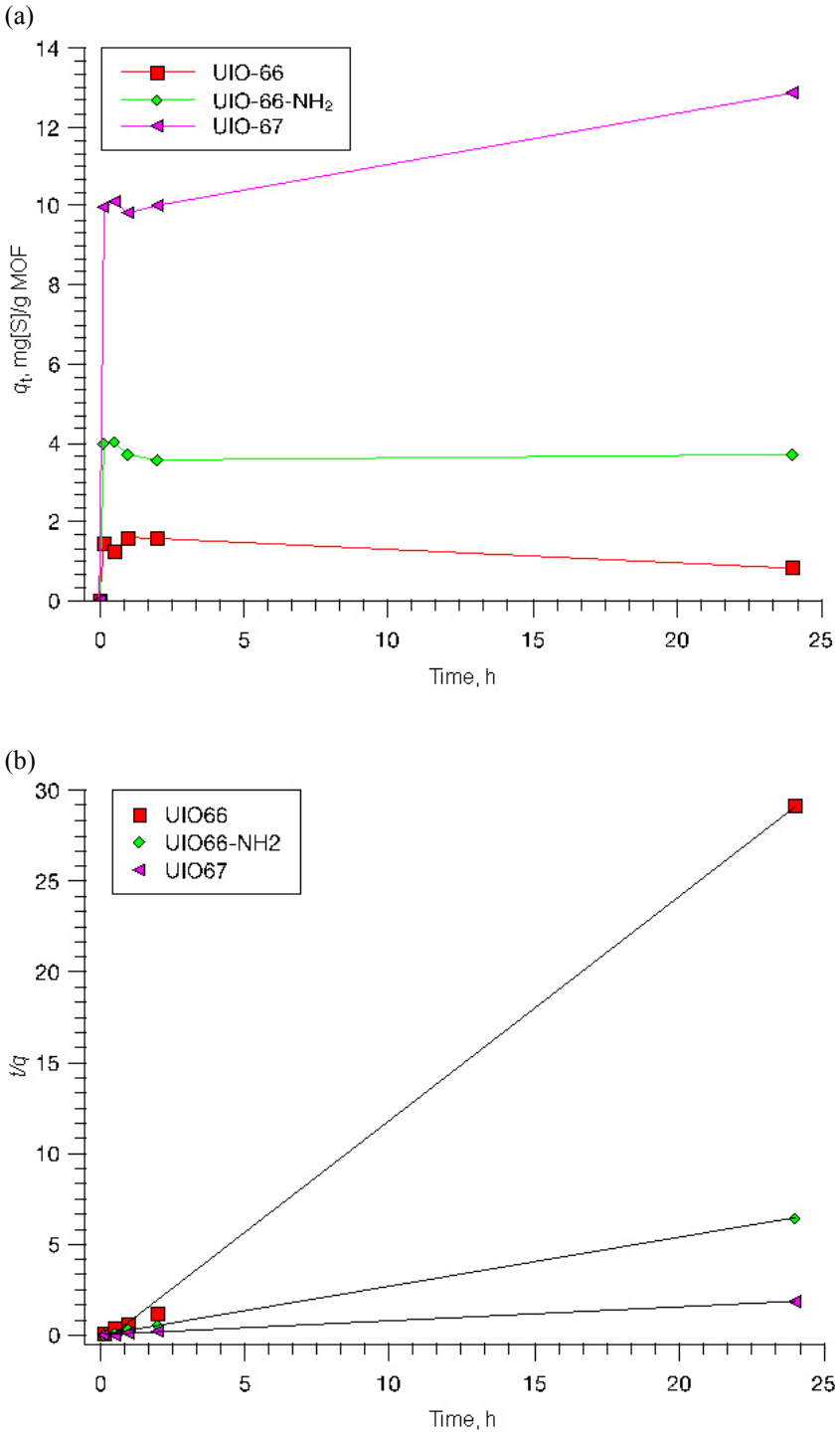

Fig. 4. (a) Kinetics of BT adsorption on selected Zr-MOFs C[S]init = 240 ppmw, (b) pseudo second-order linear kinetic plots.

3.2. BT adsorption isotherms

To assess the maximum uptake of benzothiophene on selected UIO-66 series MOFs, a sample of solid material (ca 5 mg) was exposed to solutions (1.4 mL) with different concentrations of BT (ca 70, 270, 550, 1050 and 2100 ppmw) in isooctane for 24 h at 20 °C under stirring (200 rpm). Then the resultant concentration of BT in the solution was measured by GC-FID and uptake calculated by Equation (3) [29, 31, 32]:

$$q_e = \frac{(C_i - C_e) \times m_{soln}}{m_{MOF}}, \quad (3)$$

where q_e is the amount of sulfur adsorbed at equilibrium, $\frac{mg}{g}$; C_i is the initial concentration of sulfur in solution, $\frac{mg}{g}$; C_e is the equilibrium concentration of sulfur in solution, $\frac{mg}{g}$; m_{soln} is the weight of solution, g; and m_{MOF} is the weight of MOF, g.

All experiments were conducted at least in duplicate and average data is presented.

From these data adsorption isotherms were constructed (Fig. 5) and the nonlinear Langmuir isotherm [31, 33] was fitted to obtain evaluations on the maximum adsorption capacity of adsorbents according to Equation (4):

$$q_e = \frac{q_m b C_e}{1 + b C_e}, \quad (4)$$

where q_m is the maximum amount adsorbed, $\frac{mg}{g}$; and b is the Langmuir binding strength coefficient, $\frac{kg}{mg}$.

The linearized form of the Langmuir isotherm (Eq. (5)) was used for comparison purposes:

$$\frac{C_e}{q_e} = \frac{1}{q_m} C_e + \frac{1}{q_m b}. \quad (5)$$

Coefficients of determination (R^2) obtained by the nonlinear fit were compared to the parameters from the 1st linear Langmuir fit and linear Freundlich fit. According to R^2 values the nonlinear fit was most accurate amongst selected adsorption models (Table 2).

To choose the best model, also the Freundlich isotherm was linearized, according to Equation (6) (Fig. 6) :

$$\ln q_e = \ln K_f + \frac{1}{n} \ln C_e, \quad (6)$$

where K_f is the empirical Freundlich coefficient describing sorption capacity, $\frac{mg^{1-\frac{1}{n}} k g^{\frac{1}{n}}}{g}$ and n is the empirical dimensionless constant related to the adsorption intensity [29].

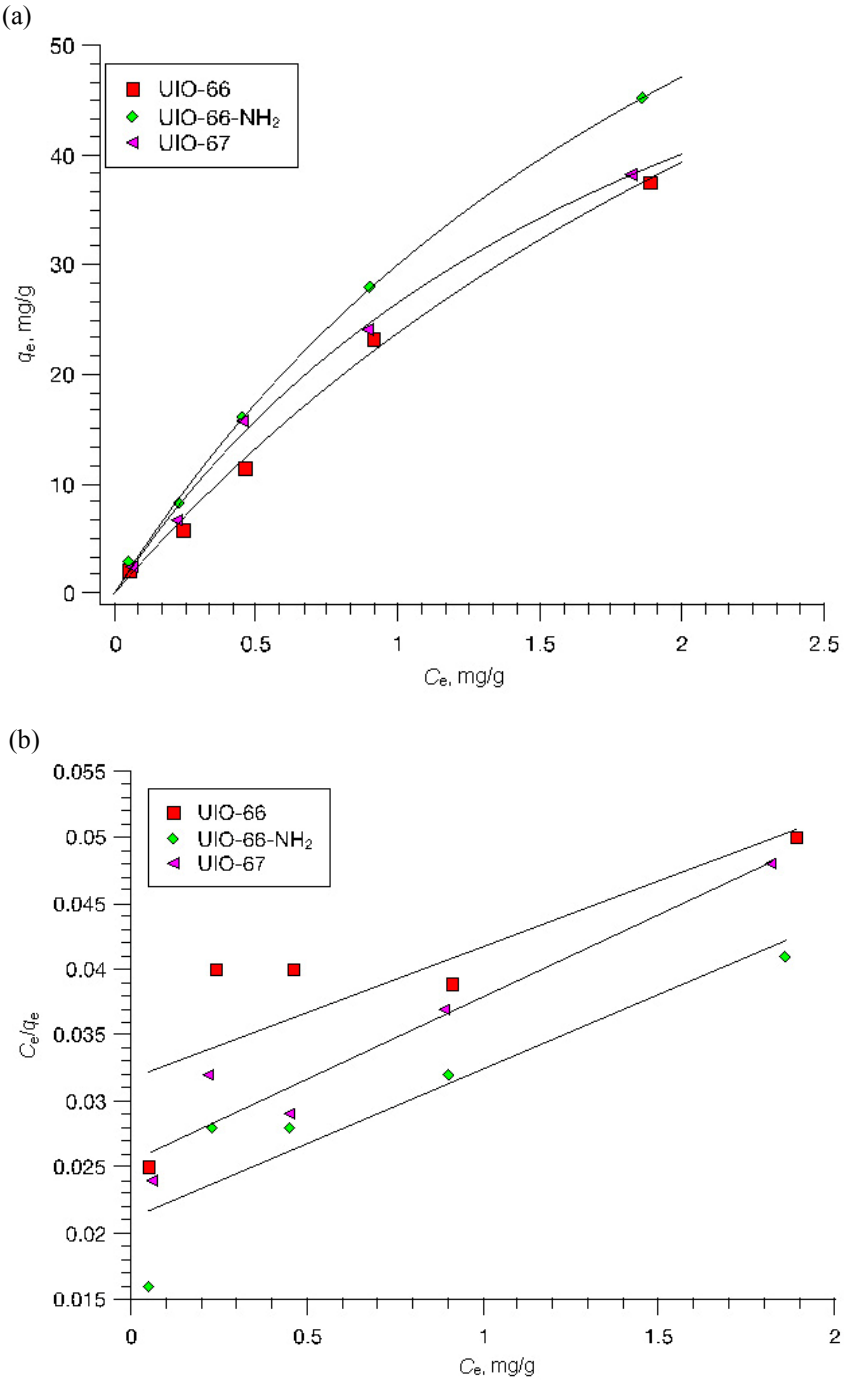

Fig. 5. BT adsorption isotherms and the corresponding nonlinear (a) and 1st linear (b) Langmuir fit.

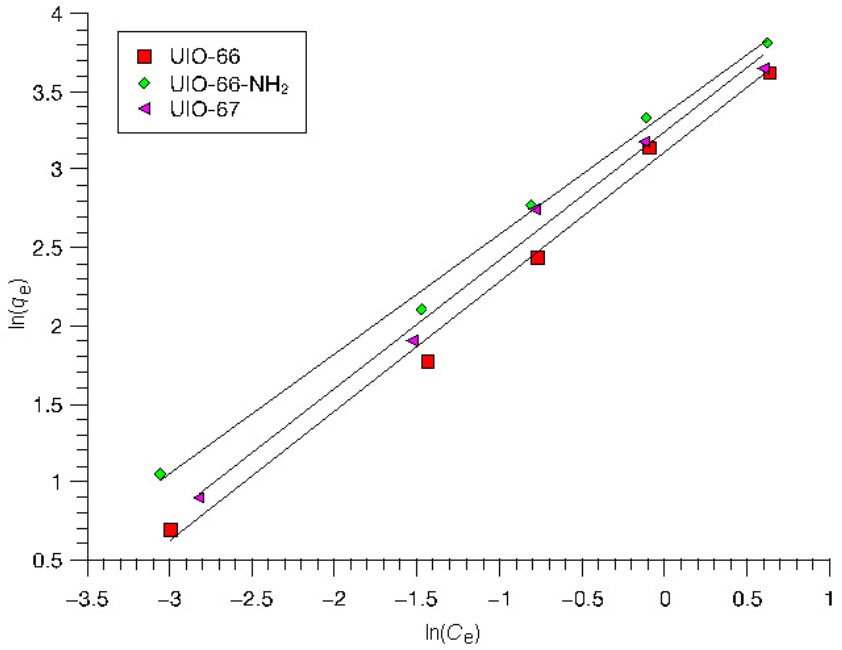

Fig. 6. Freundlich linearization of BT isotherms.

Table 2. Parameters obtained from the nonlinear Langmuir fit, 1st linear Langmuir fit and linear Freundlich fit

		Nonlinear Langmuir			1st linear Langmuir			Linear Freundlich		
No.	MOF	q_m, mg/g	b, g/mg	R^2	q_m, mg/g	b, g/mg	R^2	K_f	1/n	R^2
1	UIO-66	114	0.26	0.996	100	0.32	0.674	26	0.82	0.991
2	UIO-66-NH_2	110	0.38	0.999	88	0.54	0.828	29	0.77	0.995
3	UIO-67	82	0.48	0.997	80	0.49	0.929	22	0.83	0.993

3.3. Stability of adsorbent

Stability was assessed by subjecting the adsorbent samples to PXRD post adsorption tests (Fig. 7) and in selected cases also SEM analysis.

In general, according to PXRD data the tested adsorbents remained crystalline, which was further supported by SEM micrographs. The exception was UIO-66-NH_2, which exhibited some loss of intensity in PXRD analysis and a slight morphology change is observable in SEM micrographs.

The efficiency of UIO-66 series MOFs tested in the current work is comparable to that of Cu-BTC [14], but is lower than that of NENU-511 [34]. The latter has proven to be one of the most effective porous structures for removal of aromatic sulfur containing compounds from model fuels. Cu-BTC and NENU-511 have q_m values of 68 mg/g and 170 mg/g, respectively.

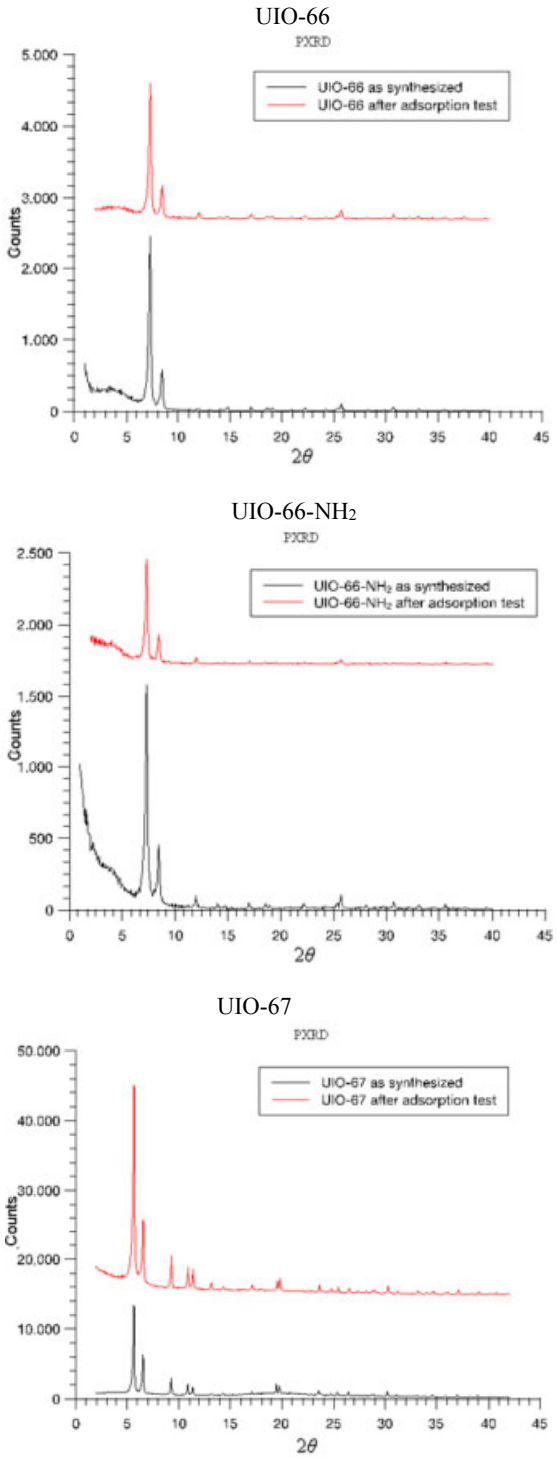

Fig. 7. Comparison of MOF samples "as synthesized" and activated to samples used for BT adsorption tests.

Figure 8 shows SEM micrographs of selected MOFs "as synthesized" and after adsorption tests.

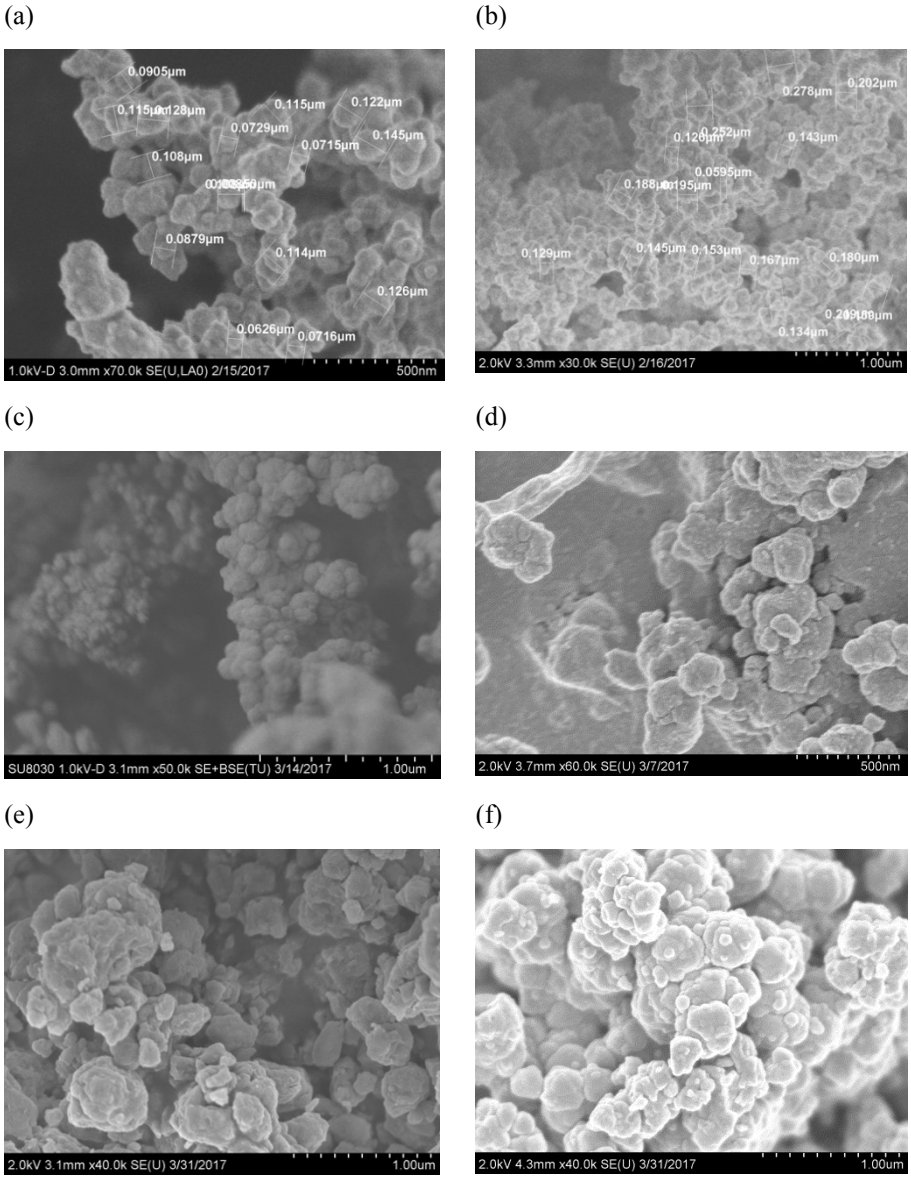

Fig. 8. SEM micrographs of selected MOFs "as synthesized" and after adsorption tests: (a) synthesized and activated UIO-66; (b) synthesized and activated UIO-66-NH_2; (c) synthesized and activated UIO-67; (d) UIO-66 after adsorption test; (e) UIO-66-NH_2 after adsorption test; (f) UIO-67 after adsorption test.

4. Conclusions

Three UIO-66 type metal-organic frameworks were synthesized and subjected to the adsorption of benzothiophene from the isooctane solution. According to the experimental results and subsequent data analysis, the examined structures measured well against Cu-BTC, although better MOF-based adsorbents were available. Also, for future experiments, flow through set-up instead of batch tests should be considered, as one of the compounds exhibited some signs of mechanical wear under mixing batch conditions.

Acknowledgements

This work made use of the Electron Probe Instrumentation Center (EPIC) facility (NUANCE Center-Northwestern University), which has received support from the MRSEC program (NSF DMR-1121262) at the Materials Research Center, and the Nanoscale Science and Engineering Center (EEC-0118025/003), both programs of the National Science Foundation, the State of Illinois; and Northwestern University and of the IMSERC at Northwestern University, which has received support from the Soft and Hybrid Nanotechnology Experimental Resource (NSF NNCI-1542205), the State of Illinois, and the International Institute for Nanotechnology. This work made also use of the J. B. Cohen X-Ray Diffraction Facility supported by the MRSEC program of the National Science Foundation (DMR-1121262) at the Materials Research Center of Northwestern University. The Author gratefully acknowledges the generous funding by Fulbright Program (Grant no. 68160328). Also, the Author gives many thanks to his hosts, Omar K. Farha and Joseph T. Hupp, during the stay at Northwestern University.

REFERENCES

1. Kreek, K., Kriis, K., Maaten, B., Uibu, M., Mere, A., Kanger, T., Koel, M. Organic and carbon aerogels containing rare-earth metals: Their properties and application as catalysts. *J. Non-Cryst. Solids*. 2014, **404**, 43–48.
2. Kamal, A., Robertson, A., Tittensor, E. Hydroxy-carbonyl compounds. Part XIV. The syntheses of some isocoumarins. *J. Chem. Soc. Resumed*, 1950, No. 0, 3375–3380. https://doi.org/10.1039/JR9500003375
3. Samokhvalov, A. Adsorption on mesoporous metal–organic frameworks in solution: Aromatic and heterocyclic compounds. *Chem. Eur. J.*, 2015, **21**(47), 16726–16742. https://doi.org/10.1002/chem.201502317
4. Khan, N. A., Jhung, S. H. Scandium-triflate/metal-organic frameworks: Remarkable adsorbents for desulfurization and denitrogenation. *Inorg. Chem.*, 2015, **54**(23), 11498–11504. https://doi.org/10.1021/acs.inorgchem.5b02118
5. Ahmed, I., Jhung, S. H. Adsorptive desulfurization and denitrogenation using metal-organic frameworks. *J. Hazard. Mater.*, 2016, **301**, 259–276. https://doi.org/10.1016/j.jhazmat.2015.08.045

6. Hu, Z., Zhao, D. *De facto* methodologies toward the synthesis and scale-up production of UiO-66-type metal–organic frameworks and membrane materials. *Dalton T.*, 2015, **44**, 19018–19040. https://doi.org/10.1039/C5DT03359D
7. Rubio-Martinez, M., Avci-Camur, C., Thornton, A. W., Imaz, I., Maspoch, D., Hill, M. R. New synthetic routes towards MOF production at scale. *Chem. Soc. Rev.*, 2017, **46**(11), 3453–3480. https://doi.org/10.1039/C7CS00109F
8. Kandiah, M., Nilsen, M. H.; Usseglio, S., Jakobsen, S., Olsbye, U., Tilset, M., Larabi, C., Quadrelli, E. A., Bonino, F., Lillerud, K. P. Synthesis and stability of tagged UiO-66 Zr-MOFs. *Chem. Mater.*, 2010, **22**(24), 6632–6640. https://doi.org/10.1021/cm102601v
9. DeCoste, J. B., Peterson, G. W., Jasuja, H., Glover, T. G., Huang, Y., Walton, K. S. Stability and degradation mechanisms of metal–organic frameworks containing the $Zr_6O_4(OH)_4$ secondary building unit. *J. Mater. Chem. A*, 2013, **1**(18), 5642–5650. https://doi.org/10.1039/C3TA10662D
10. Liu, X., Demir, N. K., Wu, Z., Li, K. Highly water-stable zirconium metal–organic framework UiO-66 membranes supported on alumina hollow fibers for desalination. *J. Am. Chem. Soc.*, 2015, **137**(22), 6999–7002. https://doi.org/0.1021/jacs.5b02276
11. Valenzano, L., Civalleri, B., Chavan, S., Bordiga, S., Nilsen, M. H., Jakobsen, S., Lillerud, K. P., Lamberti, C. Disclosing the complex structure of UiO-66 metal organic framework: A synergic combination of experiment and theory. *Chem. Mater.*, 2011, **23**(7), 1700–1718. https://doi.org/10.1021/cm1022882
12. Krtschil, U., Hessel, V., Kost, H.-J., Reinhard, D. Kolbe-Schmitt flow synthesis in aqueous solution – from lab capillary reactor to pilot plant. *Chem. Eng. Technol*,. 2013, **36**(6), 1010–1016. https://doi.org/10.1002/ceat.201200633
13. Tomás, R. A. F., Bordado, J. C. M., Gomes, J. F. P. *p*-Xylene oxidation to terephthalic acid: A literature review oriented toward process optimization and development. *Chem. Rev.*, 2013, **113**(10), 7421–7469. https://doi.org/10.1021/cr300298j
14. Li, J.-R., Sculley, J., Zhou, H.-C. Metal–organic frameworks for separations. *Chem. Rev.*, 2012, **112**(2), 869–932. https://doi.org/10.1021/cr200190s
15. Farrusseng, D., Aguado, S., Pinel, C. Metal–organic frameworks: opportunities for catalysis. *Angew. Chem. Int. Edit.*, 2009, **48**(41), 7502–7513. https://doi.org/10.1002/anie.200806063
16. Crombie, L., Games, D. E., James, A. W. G. Reactions of fused and unfused α-pyrones with magnesium alkoxide, sodium alkoxide and water as the nucleophile: effects of chelation. *J. Chem. Soc., Perk. 1*, 1996, 22, 2715–2724. https://doi.org/10.1039/P19960002715
17. Qu, R.-Y., Liu, Y.-C., Wu, Q.-Y., Chen, Q., Yang, G.-F. An efficient method for syntheses of functionalized 6-bulkysubstituted salicylates under microwave irradiation. *Tetrahedron*, 2015, **71**(42), 8123–8130. https://doi.org/10.1016/j.tet.2015.08.040
18. Fadzil, N. A. M., Rahim, M. H. A., Maniam, G. P. A brief review of *para*-xylene oxidation to terephthalic acid as a model of primary C–H bond activation. *Chinese J. Catal.*, 2014, **35**(10), 1641–1652. https://doi.org/10.1016/S1872-2067(14)60193-5
19. Wuensch, C., Glueck, S. M., Gross, J., Koszelewski, D., Schober, M., Faber, K. Regioselective enzymatic carboxylation of phenols and hydroxystyrene

derivatives. *Org. Lett.*, 2012, **14**(8), 1974–1977. https://doi.org/10.1021/ol300385k

20. Wuensch, C., Schmidt, N., Gross, J., Grischek, B., Glueck, S. M., Faber, K. Pushing the equilibrium of regio-complementary carboxylation of phenols and hydroxystyrene derivatives. *J. Biotechnol.*, 2013, **168**(3), 264–270. https://doi.org/10.1016/j.jbiotec.2013.07.017
21. Harris, C. M., Kibby, J. J., Fehlner, J. R., Raabe, A. B., Barber, T. A., Harris, T. M. Amino acid constituents of ristocetin A. *J. Am. Chem. Soc.*, 1979, **101**(2), 437–445. https://doi.org/10.1021/ja00496a028
22. Sakurai, J., Kikuchi, T., Takahashi, O., Watanabe, K., Katoh, T. Enantioselective total synthesis of (+)-stachyflin: A potential anti-influenza A virus agent isolated from a microorganism. *Eur. J. Org. Chem.*, 2011, **2011**(16), 2948–2957. https://doi.org/10.1002/ejoc.201100173
23. Katz, M. J., Brown, Z. J., Colon, Y. J., Siu, P. W., Scheidt, K. A., Snurr, R. Q., Hupp, J. T., Farha, O. K. A facile synthesis of UiO-66, UiO-67 and their derivatives. *Chem. Commun.* 2013, **49**(82), 9449–9451. https://doi.org/10.1039/C3CC46105J
24. Rimoldi, M., Howarth, A. J., De Stefano, M. R., Lin, L., Goswami, S., Li, P., Hupp, J. T., Farha, O. K. Catalytic zirconium/hafnium-based metal–organic frameworks. *ACS Catal.*, 2017, **7**(2), 997–1014. https://doi.org/10.1021/acscatal.6b02923
25. Wang, C., Volotskova, O., Lu, K., Ahmad, M., Sun, C., Xing, L., Lin, W. Synergistic assembly of heavy metal clusters and luminescent organic bridging ligands in metal–organic frameworks for highly efficient X-ray scintillation. *J. Am. Chem. Soc.*, 2014, **136**(17), 6171–6174. https://doi.org/10.1021/ja500671h
26. Cliffe, M. J., Wan, W., Zou, X., Chater, P. A., Kleppe, A. K., Tucker, M. G., Wilhelm, H., Funnell, N. P., Coudert, F.-X., Goodwin, A. L. Correlated defect nanoregions in a metal–organic framework. *Nat. Commun.*, 2014, **5**(1), 4176–4183.
27. Shearer, G. C., Chavan, S., Bordiga, S., Svelle, S., Olsbye, U., Lillerud, K. P. Defect engineering: Tuning the porosity and composition of the metal–organic framework UiO-66 via modulated synthesis. *Chem. Mater.*, 2016, **28**(11), 3749–3761. https://doi.org/10.1021/acs.chemmater.6b00602
28. Ho, Y.-S. Second-order kinetic model for the sorption of cadmium onto tree fern: A comparison of linear and non-linear methods. *Water Res.*, 2006, **40**(1), 119–125. https://doi.org/10.1016/j.watres.2005.10.040
29. Nouri, L., Ghodbane, I., Hamdaoui, O., Chiha, M. Batch sorption dynamics and equilibrium for the removal of cadmium ions from aqueous phase using wheat bran. *J. Hazard. Mater.*, 2007, **149**(1), 115–125. https://doi.org/10.1016/j.jhazmat.2007.03.055
30. Van de Voorde, B., Hezinova, M., Lannoeye, J., Vandekerkhove, A., Marszalek, B., Gil, B., Beurroies, I., Nachtigall, P., De Vos, D. Adsorptive desulfurization with CPO-27/MOF-74: an experimental and computational investigation. *Phys. Chem. Chem. Phys.*, 2015, **17**(16), 10759–10766. https://doi.org/ 10.1039/C5CP01063B
31. Bolster, C. H., Hornberger, G. M. On the use of linearized Langmuir equations. *Soil Sci. Soc. Am. J.* **2007**, **71**(6), 1796–1806. https://doi.org/10.2136/sssaj2006.0304

32. Bagheri, M., Masoomi, M. Y., Morsali, A. High organic sulfur removal performance of a cobalt based metal-organic framework. *J. Hazard. Mater.*, 2017, **331**, 142–149. https://doi.org/10.1016/j.jhazmat.2017.02.037
33. Zuyi, T., Taiwei, C. On the applicability of the Langmuir equation to estimation of adsorption equilibrium constants on a powdered solid from aqueous solution. *J. Colloid Interf. Sci.*, 2000, **231**(1), 8–12. https://doi.org/10.1006/ jcis.2000.7057
34. He, W.-W., Yang, G.-S., Tang, Y.-J., Li, S.-L., Zhang, S.-R.; Su, Z.-M., Lan, Y.-Q. Phenyl groups result in the highest benzene storage and most efficient desulfurization in a series of isostructural metal–organic frameworks. *Chem. Eur. J.*, 2015, **21**(27), 9784–9789. https://doi.org/10.1002/ chem. 201500815

Received December 18, 2018